The Veterinary Journal 206 (2015) 338–348

Contents lists available at ScienceDirect

The Veterinary Journal

journal homepage: www.elsevier.com/locate/tvjl

Systematic arthroscopic investigation of the bovine stifle joint

U. Hagag [a,b,*], M.G. Tawfiek [c], W. Brehm [a]

[a] Large Animal Clinic for Surgery, Faculty of Veterinary Medicine, University of Leipzig, Leipzig, Germany
[b] Department of Surgery, Anesthesiology, and Radiology, Faculty of Veterinary Medicine, Beni-Suef University, Beni-Suef 62511, Egypt
[c] Department of Anatomy and Embryology, Faculty of Veterinary Medicine, Beni-Suef University, Beni-Suef 62511, Egypt

ARTICLE INFO

Article history:
Accepted 6 September 2015

Keywords:
Cattle
Stifle
Surgery
Arthroscopy
Anatomy

ABSTRACT

The objective of the present study was to establish a protocol for arthroscopic exploration of the bovine stifle joint using craniomedial, caudolateral and caudomedial approaches. An anatomic and arthroscopic study using 26 cadaveric limbs from 13 non-lame adult dairy cows was performed. The craniomedial approach was created between the middle and medial patellar ligaments to investigate the cranial pouches of the stifle joint. The inter-condylar eminence, the proximal aspect of the medial femoral trochlear ridge and the lateral aspect of the lateral femoral condyle were used as starting points for systematic examination of the medial femorotibial, the femoropatellar and the lateral femorotibial joints, respectively.

The observed structures were: the suprapatellar pouch, articular surfaces of the patella, femoral trochlear ridges, cruciate ligaments, menisci, and the meniscotibial ligaments. The arthroscopic portal for the caudomedial femorotibial pouch was about 6–8 cm caudal to the medial collateral ligament. The proximal and distal caudolateral femorotibial pouches were explored 3 cm and 1.5 cm caudal to the ipsilateral collateral ligament, respectively. The observed structures were the caudal aspect of femoral condyles, menisci, caudal cruciate ligament, popliteal tendon and the meniscofemoral ligament. Restricted joint size and risk of common peroneal nerve damage were the major limitations for exploration of the caudal femorotibial compartments. The study described the arthroscopic portals and normal intra-articular anatomy of the bovine stifle joint but further investigations are warranted to validate these techniques in clinical cases.

Introduction

Lameness originating from the stifle joint is relatively common in cattle (Ducharme et al., 1985; Pentecost and Niehaus, 2014). The complex arrangement of osseous, articular, fibro-cartilaginous and ligamentous structures and the biomechanics of the stifle joint during motion as well as hereditary factors in certain breeds were suggested to be predisposing factors in stifle lameness (Ducharme et al., 1985). Disorders of the bovine stifle include fractures, septic arthritis, traumatic arthritis with injuries of the menisci, collateral, meniscal and/or cruciate ligaments and osteoarthritis (Hurtig, 1985; Munroe and Cauvin, 1994; Gaughan, 1996; Trostle et al., 1997; Tryon and Farrow, 1999).

Radiography, ultrasonography, magnetic resonance tomography (MRT) and computed tomography (CT) have been used in bovine orthopaedics (Kofler et al., 2014). The bovine stifle joint has been thoroughly examined with radiography and ultrasonography (Kofler, 1999; Siegrist and Geissbuehler, 2011) but radiography provides little information on soft tissue structures and ultrasonography is limited to bone surfaces. CT and MRT are valuable diagnostic imaging modalities, but their use in cattle is limited to advanced veterinary clinics due to the high cost and the need for general anaesthesia (Lee et al., 2009; Ehlert et al., 2011; Nuss et al., 2011).

Arthroscopy and arthrotomy offer valuable information for diagnosis and treatment of stifle joint injuries (Hurtig, 1985; Plesman et al., 2013). Arthroscopy is superior to arthrotomy because of the minimal damage to the peri-articular soft tissues, multiple joint approaches, smaller incisions, short operative times, improved intra-articular visibility, enhanced cosmetic appearance, and rapid recovery (Honnas et al., 1993; Necas et al., 2002). In addition, arthroscopy allows examination of structures within the joint that are inaccessible with routine arthrotomy (Honnas et al., 1993; Lardé and Nichols, 2014); however, arthroscopy is not widely used in cattle due to cost and availability, so its use is limited to valuable cows and breeding bulls (Lardé and Nichols, 2014).

The bovine stifle consists of the femoropatellar (FP), medial femorotibial (MFT), and lateral femorotibial (LFT) joints (Dyce and Wensing, 1971; Ashdown and Done, 1984; Nickel et al., 1985; Desrochers et al., 1996; Lopez et al., 1996; Budras et al., 2003; Dyce et al., 2010). The FP and MFT joints always communicate, while the MFT and LFT joints communicate in 57% of bovine stifles (Desrochers et al., 1996).

The cranial arthroscopic approach to the stifle joint has been reported in cattle (Hurtig, 1985; Munroe and Cauvin, 1994; Lardé and Nichols, 2014; Nichols and Anderson, 2014), horse (Martin and

* Corresponding author. Tel.: +20 822327982.
E-mail address: usamahagag@yahoo.de (U. Hagag).

http://dx.doi.org/10.1016/j.tvjl.2015.09.006
1090-0233/

McIlwraith, 1985; Moustafa et al., 1987; Vinardell et al., 2008), dog (Marino and Loughin, 2010), South American camelids (Pentecost et al., 2012) and sheep (Modesto et al., 2014). Although the caudal approaches to the femorotibial (FT) joints have been described in horses (Watts and Nixon, 2006) and sheep (Modesto et al., 2014), reports on the arthroscopic evaluation of the caudal FT pouches in bovine are lacking. Consequently, the objective of the current study was to develop a satisfactory technique for arthroscopic examination of the FT and FP joints in cattle and to establish a protocol for exploration and characterization of the cranial and caudal aspects of the FT joints to provide a detailed systematic description of the intra-articular structures of the bovine stifle joint.

Materials and methods

Study design

Pelvic limbs (26) from (13) adult Holstein–Friesian cow cadavers euthanased for reasons unrelated to orthopaedic disease were evaluated. Arthroscopic exploration of 22 stifles was performed (12 cranial and 10 caudal compartments) and four stifles were dissected in detail to demonstrate the regional anatomy. The animals' ages ranged from 3 to 12 years (mean 3 years) with weights ranging from 400 to 600 kg (mean 475 kg). The limbs were disarticulated at the hip joint, stored at –20 °C, and thawed at room temperature for all procedures. Anatomical evaluations were performed via gross dissection, computed tomography and arthroscopy.

Anatomical study

A gross dissection was performed in four limbs to determine the anatomical landmarks for the arthroscopic portals, the intra-articular structures and the communication between the FT and FP compartments. In order to ensure correct identification of the anatomical structures seen arthroscopically, long spinal needles (Spinocan 22G × 180 mm, B. Braun) were placed into each tissue under arthroscopic guidance, and tissue identity was confirmed with subsequent dissection.

Gross dissection was performed at the end of each procedure to determine entry site and structures penetrated during portal creation. Fluid extravasation and iatrogenic damage to the articular surfaces were observed and recorded.

Computed tomography (CT)

Survey CT scans were performed on three cadavers using a 16-detector row helical scanner (Philips Mx8000 IDT 16-slice helical CT scanner). The acquisition settings were: 120 kV, 400 mA, slice thickness of 1 mm, slice increment of 0.6 mm, rotation time of 1 s, pitch of 0.635, scan field of view of 45 cm, window width of 2000 and window level of 500 Hounsfield Units and matrix size of 512 × 512 pixels. Reconstruction of the transverse images was performed and a three-dimensional image was created to illustrate the relationships between the osseous and soft tissue structures of the stifle joint (Figs. 1–3).

Arthroscopy

Instruments

A 4 mm diameter and 30° angle view arthroscope (Storz) was used to evaluate the three compartments of stifle joint. Continuous joint irrigation and distension were maintained using an Arthroflow (Ormed) system. A fibre optic light cable connected to a 175 W, xenon light source (Karl Storz Endovision) was attached to the arthroscope to provide joint illumination. Representative images and videos were recorded for later review (Aida Vet DVD, Karl Storz Endovision).

Cadaver positioning and preparation

Limbs were tied just below the fetlock joint, elevated and positioned as if the animal was in dorsal recumbency using an overhead hoist. The arthroscopic sleeve and conical obturator were manipulated into the MFT with the stifle joint in 120° of flexion. The cranial and caudal compartments of the FT joints were examined with the stifle joint in 90° of flexion. Limbs were secured in position via a metal frame attached medially and laterally to the thigh region. The stifle region was clipped of hair and cleaned.

Joint distension

Due to the communication between the three compartments of the stifle joint in most instances (nine cadavers), joint distension was achieved through needle insertion into the craniomedial FT joint. An 18 G needle was inserted approximately 1–2 cm cranial to the medial collateral ligament, halfway between the medial tibial plateau and medial femoral condyle. The joint was distended with 30–60 mL saline solution until the joint pouch was visibly distended and there was mild resistance to injection. In three cadavers, the cranial LFT and MFT pouches appeared to be separated by a synovial septum and distension of the LFT joint was achieved via 30–60 mL saline using an 18 G needle inserted between the lateral and middle patellar ligaments.

Surgical procedure

Cranial FT and FP joints

Using a number 15 scalpel blade a 1 cm incision was created through the skin and fascia between the middle and medial patellar ligaments halfway between the tibial crest and the distal aspect of the patella. The arthroscopic sleeve and conical

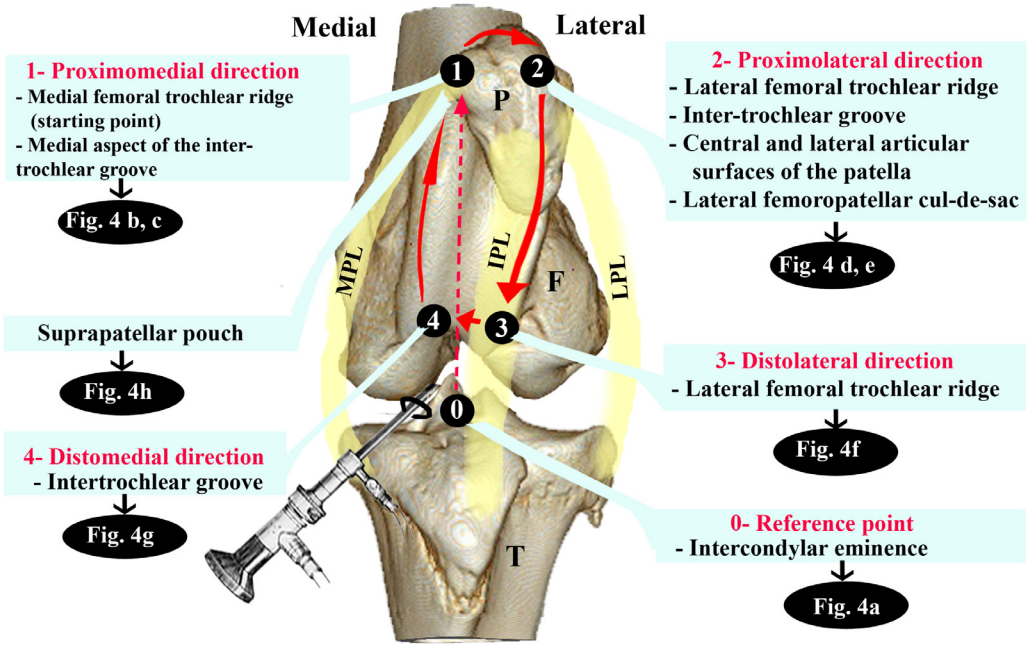

Fig. 1. Computer tomographic image of a left stifle illustrating the arthroscopic approach to the femoropatellar joint using a craniomedial arthroscopic portal (between the middle and medial patellar ligaments). Red arrows indicate the direction of the arthroscope (0–4) within the joint cavity. The intra-articular structures viewed during the arthroscopic investigation and their figure numbers are listed. P, patella; F, femur; T, tibia; MPL, medial patellar ligament; IPL, intermediate patellar ligament; LPL, lateral patellar ligament.

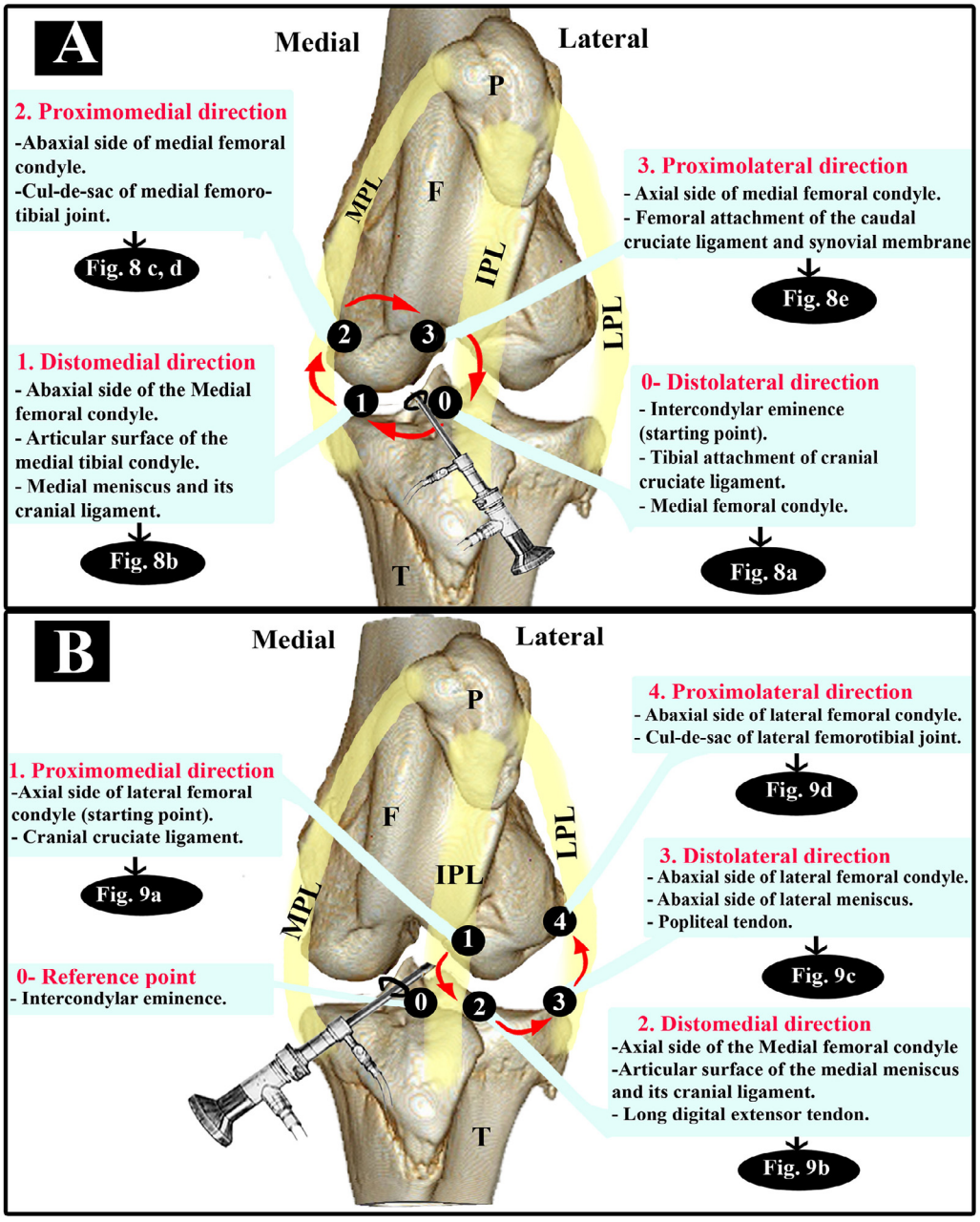

Fig. 2. Computer tomographic image of a left stifle demonstrating the arthroscopic approach to the cranial compartments of the medial (A) and lateral (B) femorotibial joints using a craniomedial arthroscopic portal (between the middle and medial patellar ligaments). Red arrows indicate the direction of the arthroscope (0–4) within the joint cavity. The intra-articular structures viewed during the arthroscopic investigation and their figure numbers are listed. P, patella; F, femur; T, tibia; MPL, medial patellar ligament; IPL, intermediate patellar ligament; LPL, lateral patellar ligament.

obturator were manipulated through the skin incision and advanced caudomedially to penetrate the MFT joint capsule. The stifle was positioned at 90° of flexion. Fluid egress from the open port of the arthroscopic sleeve confirmed joint penetration. When the sleeve was positioned to the hilt, the obturator was removed and replaced with the arthroscope. The inter-condylar eminence was located and used as a reference point (Fig. 4a). As the MFT and FP joints communicate, the arthroscope was gently manipulated and advanced in a caudomedial direction from the intercondylar eminence (MFT joint) towards the FP joint beneath the patella and over the femoral trochlea (Fig. 1).

Once the FP joint was investigated, the arthroscope was withdrawn to the intercondylar eminence to examine the cranial MFT compartment (Fig. 2A). In nine cadavers, investigation of the LFT joint was achieved directly by advancing the arthroscope in a caudolateral direction towards the lateral femoral condyle (Fig. 2B). In three cadavers, a synovial membrane appeared to separate the MFT and LFT compartments. In those limbs, the telescope was replaced by the conical obturator. The obturator and sleeve were then inserted to their full extent through this membrane in a caudolateral direction. The obturator was removed and replaced with the arthroscope and the LFT pouch was systematically explored.

Caudal FT compartments

To explore the caudal FT compartments, joint distension was achieved as described for the cranial compartments. Before skin incision, a 3.5 inch (89 mm) spinal needle was always inserted to verify the direction of insertion and successful distension of the caudal pouches. The spinal needle was directed axially, cranially, and proximally.

The arthroscopic portal for the caudomedial FT pouch was about 6–8 cm caudal to the medial collateral ligament, 1 cm proximal to the level of a line between the palpable tibial tuberosity and tibial condyle, 1–2 cm cranial to the medial saphenous vein, and cranioproximal to the palpable gracilis muscle, with the limb in 90° of flexion (Fig. 3A).

The arthroscopic portal for the proximal caudolateral FT pouch was 2 cm proximal to the tibial plateau and 3 cm caudal to the lateral collateral ligament. To examine

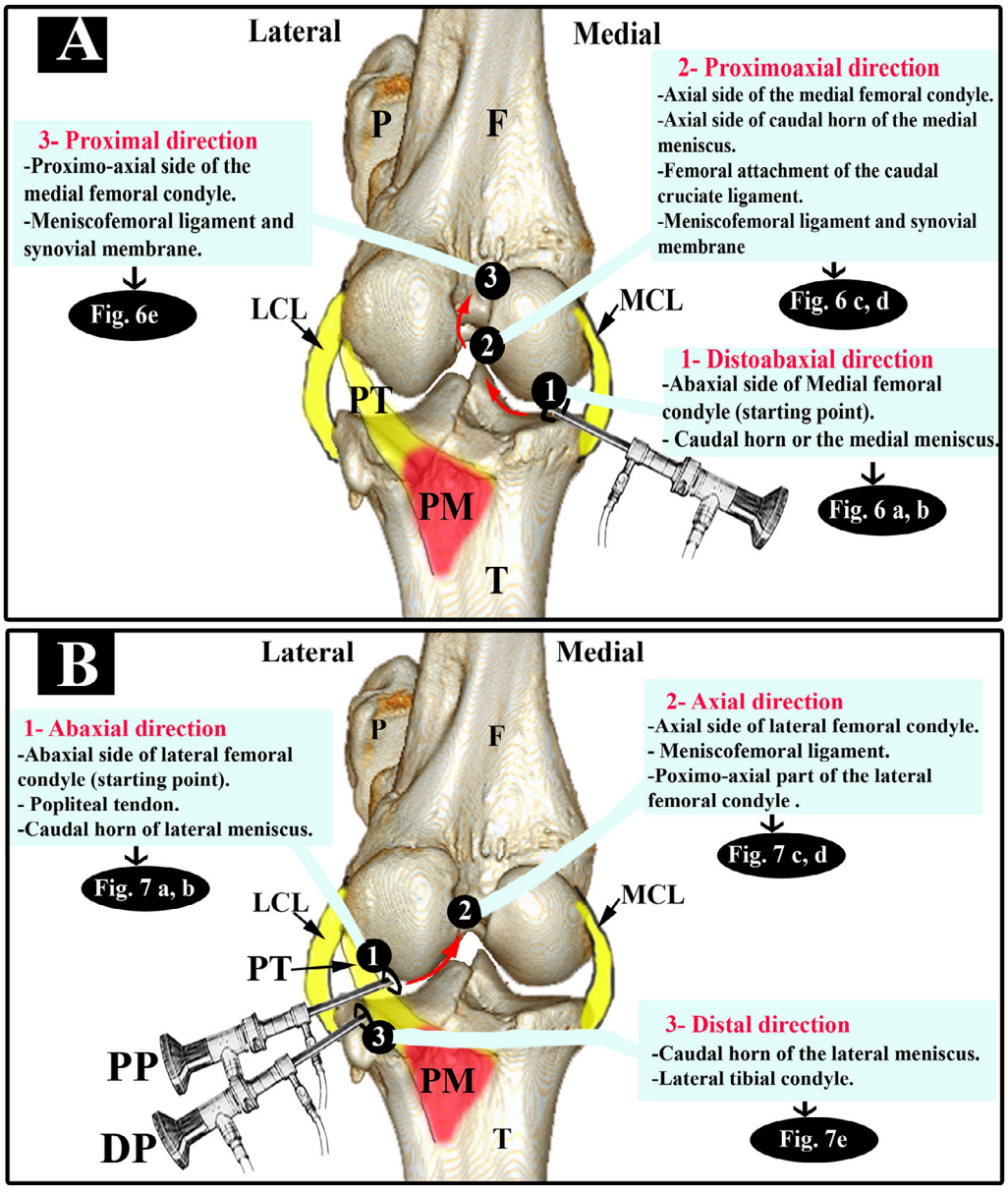

Fig. 3. Computer tomographic image of a left stifle demonstrating the arthroscopic approaches to the caudal compartments of the medial (A) and lateral (B) femorotibial joints together with the intra-articular arthroscopic directions (1–3). (A) The caudomedial arthroscopic portal was 6–8 cm caudal to the medial collateral ligament (MCL). (B) The caudolateral arthroscopic portal was 3 cm caudal to the lateral collateral ligament (LCL), 2 cm proximal to the tibial plateau for the proximal pouch (PP) and 1 cm for the distal pouch (DP) entry in cranial. The intra-articular structures viewed during the arthroscopic investigation and their figure numbers are listed. PM, popliteal muscle; PT, popliteal tendon; P, patella; F, femur; T, tibia.

the distal caudolateral pouch, the portal was located 1 cm proximal to the tibial plateau and 1.5 cm caudal to the lateral collateral ligament (Fig. 3B).

A 5 mm vertical stab incision was made through the skin, fascia and aponeurosis of the flexor musculature followed by insertion of the arthroscopic sleeve and blunt obturator in the same direction as the spinal needle. The arthroscope then replaced the obturator and the joint was systematically explored. Fluid egress was achieved via an 18 G needle inserted between middle and medial patellar ligaments.

Results

Cadaver dissection

Gross dissection of four stifle joints demonstrated the palpable structures used as landmarks during the arthroscopic entry procedure (Fig. 5). It was hard to palpate the collateral ligaments, the lateral patellar ligament was completely blended with the biceps femoris tendons and the medial collateral ligament was firmly attached to the medial meniscus. In three cadavers, the MFT, FP and LFT joint cavities communicated and in one specimen the cranial MFT and LFT joints were separated by a thin membrane. No essential neurovascular structures were observed that could be damaged during the craniomedial arthroscopic approach to the bovine stifle joint.

In the caudal FT joints, the common peroneal nerve and popliteal artery and vein were identified as neurovascular structures vulnerable to iatrogenic injury (Figs. 6,7). The common peroneal nerve traced across the lateral head of the gastrocnemius muscle and deep to the biceps femoris muscle. The location of the common peroneal nerve overlying the caudal LFT compartment was variable. When the limb was extended, the nerve was as close as 3 cm caudal to the lateral collateral ligament, and became even closer as it coursed more distally. When the limb was flexed during dissection, the nerve was

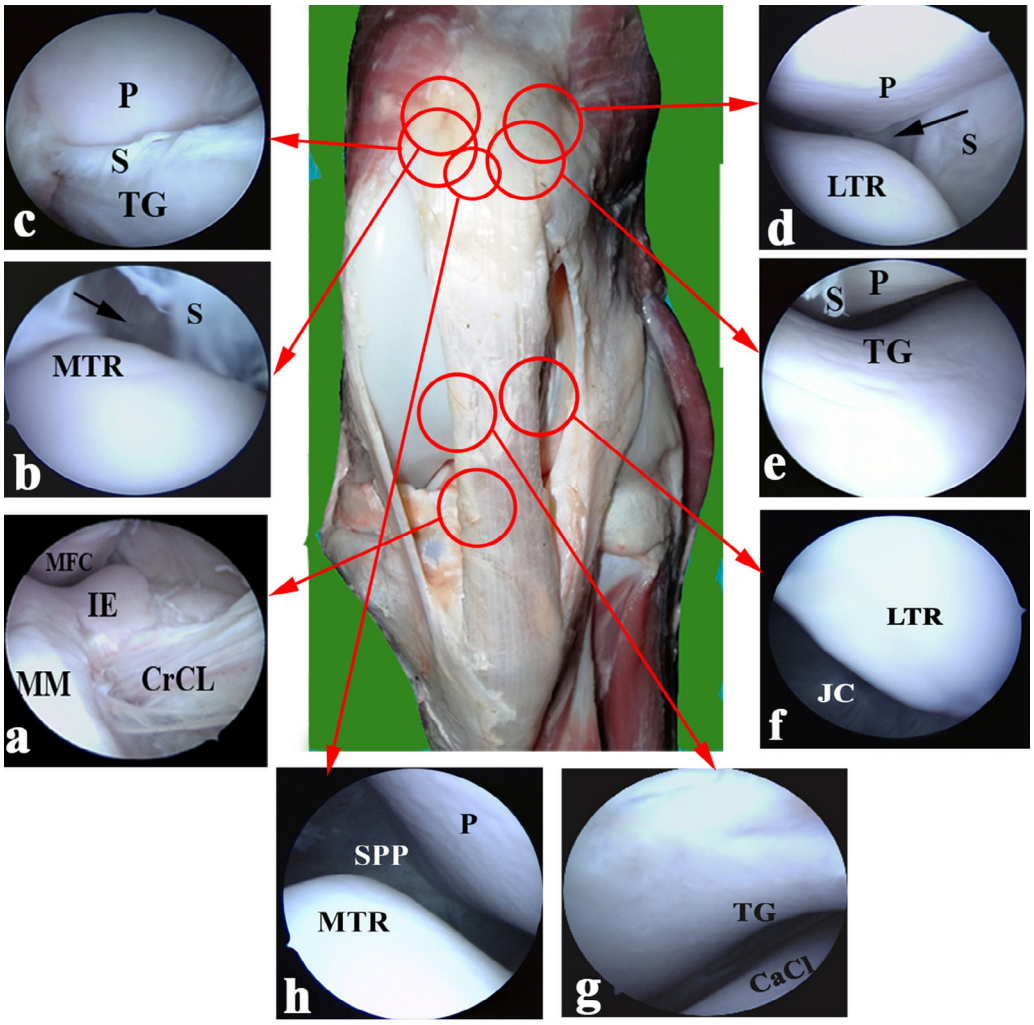

Fig. 4. Arthroscopic views of the femorotibial joint (a) and the femoropatellar joint (b, c, d, e, f, g, h) using the craniomedial arthroscopic approach in Fig. 1. Visual areas of the arthroscope identified with red circles on gross dissection of the cranial aspect of the left stifle joint. (a) Inter-condylar eminence (IE) reference point with bundles of the tibial attachment of the cranial cruciate ligament (CrCL); axial part of cranial horn of the medial meniscus (MM) and axial side of the medial femoral condyle (MFC). (b) Close-up view with the arthroscope over the medial trochlear ridge of the femur (MTR) showing the synovial membrane (S) lining the suprapatellar pouch (black arrow). (c) Close-up view with the arthroscope under the patella (P) at the level of the medial aspect of the femoral trochlear groove (TG) closely related to the patella and covered by synovial membrane (S). (d) Arthroscopic view of the lateral trochlear ridge (LTR); lateral part of the patella (P) and the synovial membrane (S) lining the lateral femoropatellar cul-de-sac (black arrow). (e) Close-up view of arthroscope under the patella (P) over the proximal femoral trochlear groove (TG); the synovial membrane (S). There is more separation between the patella and the lateral side of the trochlear groove. (f) Close-up view of arthroscope at the distal aspect of lateral trochlear ridge of the femur (LTR) above the femorotibial joint cavity (JC). (g) Arthroscopic view of the distal aspect of the femoral trochlear groove (TG) and the most proximal part of the femoral attachment of the caudal cruciate ligament (CaCl). (h) Increased illumination to investigate the suprapatellar pouch (SPP), with a clear patellar surface (P) and medial trochlear ridge of the femur (MTR).

located about 7–8 cm caudal to the lateral collateral ligament at the level of the mid-femoral condyle. The popliteal tendon originated from the lateral femoral epicondyle, passed intra-articularly under the lateral collateral ligament and exited the FT joint at its caudolateral aspect. The popliteal tendon divided the caudolateral compartment of the FT joint into proximal and distal pouches (Figs. 5c,7).

Dissection of stifles following arthroscopy revealed substantial subcutaneous and intermuscular fluid accumulation around the portal of arthroscopic entry. Iatrogenic cartilage damage was observed at the apex and on the articular surfaces of the patella (two stifles) and in the articular cartilage of the caudal compartments (three stifles), but the lesion was considered small and superficial enough to be of limited concern.

Arthroscopy

Arthroscopic examination of the stifle joint was initially achieved in approximately 65 min for the cranial compartments and approximately 45 min for the caudal compartments. After standardization of the technique, the ability to evaluate the joint structures was progressively improved due to increased surgical proficiency. By the end of the study, the duration of examination was approximately 45 min for the cranial compartments and approximately 30 min for the caudal compartments of the stifle joint. The intra-articular orientation terms of the arthroscope were described and illustrated with reference to the animal in standing position (Figs. 1–3). Synovial reflux and the ability to freely move the sleeve were reliable indicators for joint entry when the arthroscope was inserted between the medial and middle patellar ligaments (Figs. 1,2).

FP joint

Starting from the reference point (inter-condylar eminence) (Fig. 4a), the arthroscope was advanced proximally and caudomedially towards the FP joint. The joint was examined in a systematic manner with exploration initiated proximomedially from

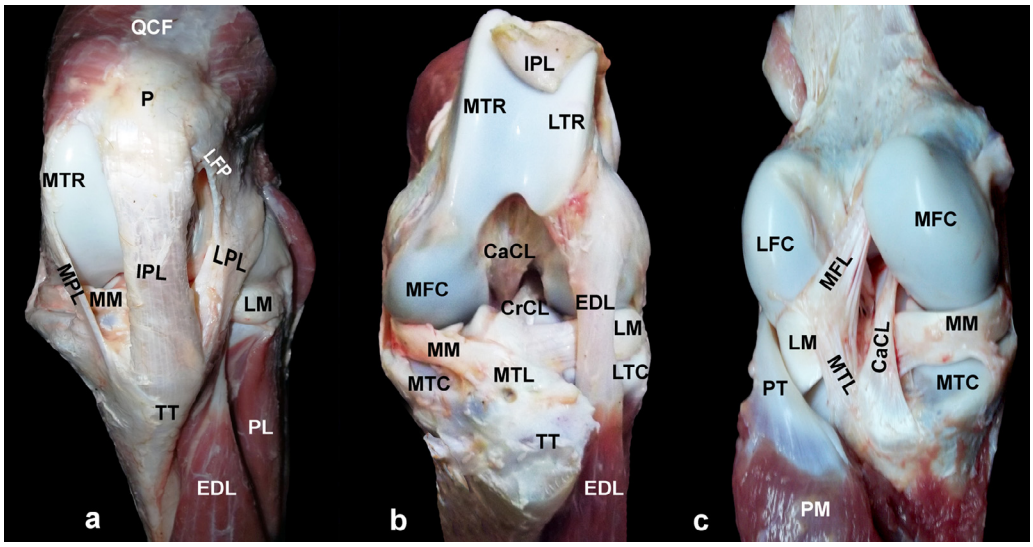

Fig. 5. Gross dissection of the left stifle joint of cattle: (a) Cranial view, the joint capsule and the infrapatellar fat pad were removed to expose the peri-articular structures on the cranial aspect of the joint. (b) Cranial view, the patella and patellar ligaments were reflected to expose the intra-articular structures on the cranial aspect of the joint. (c) Caudal view of the femorotibial joint in extension, after removal of the gastrocnemius muscle and joint capsule to expose the peri-articular structures on the caudal aspect of the joint. CaCL, caudal cruciate ligament; CrCl, cranial cruciate ligament; EDL, long digital extensor muscle and tendon; IPL, intermediate (middle) patellar ligament; LFC, lateral femoral condyle; LFP, lateral femoropatellar ligament; LM, lateral meniscus; LPL, lateral patellar ligament; LTC, lateral tibial condyle; LTR, lateral trochlear ridge of the femur; MFC, medial femoral condyle; MFL, meniscofemoral ligament; MM, medial meniscus; MTC, medial tibial condyle; MTL, meniscotibial ligament; MTR, medial trochlear ridge of the femur; MPL, medial patellar ligament; P, patella; PL, peroneus longus muscle; PM, popliteus muscle; PT, popliteal tendon; TT, tibial tuberosity; QCF, quadriceps femoris muscle.

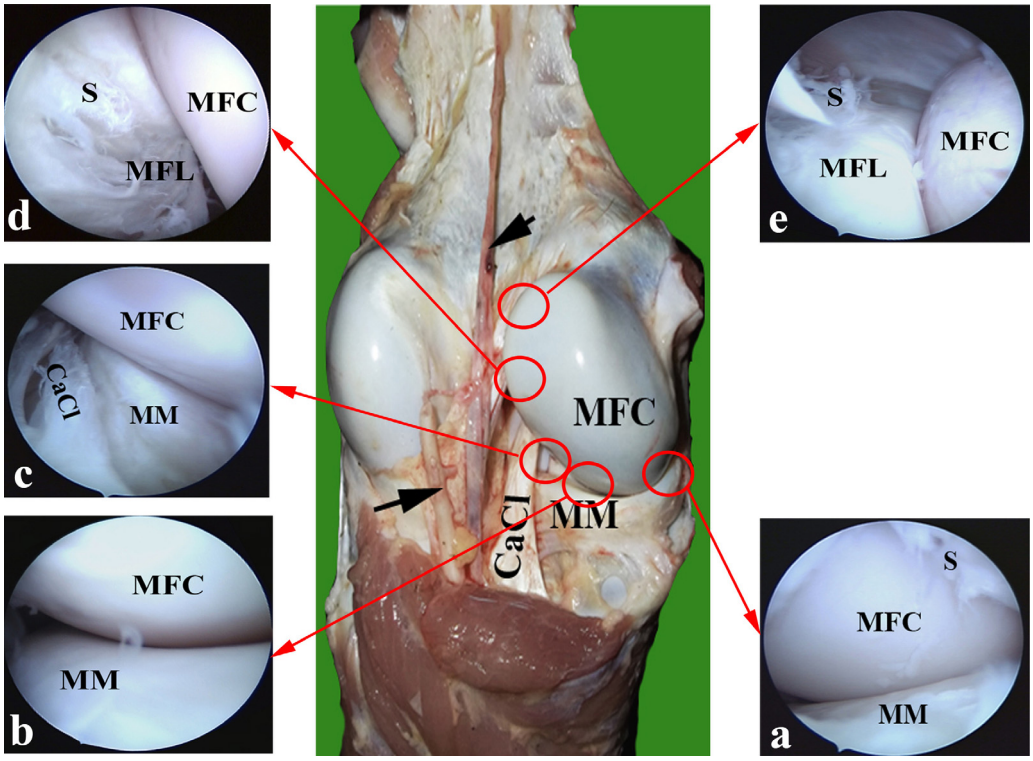

Fig. 6. Arthroscopic views of the caudal compartment of the medial femorotibial joint (a, b, c, d, e) using the caudomedial arthroscopic approach in Fig. 3A. Visual areas of the arthroscope identified with red circles on gross dissection of the caudal aspect of the left stifle joint; (MFC) medial femoral condyle; (MM) caudal horn of the medial meniscus (CaCL); caudal cruciate ligament; (black arrows) the vital neurovascular structures. (a) Abaxial side of the medial femoral condyle (MFC) over the articular surface of the caudal horn of the medial meniscus (MM) with lining synovial membrane (S). (b) Caudal aspect of the medial femoral condyle (MFC) over the articular surface of the caudal horn of the medial meniscus (MM). (c) Disto-axial side of the medial femoral condyle (MFC) over the articular surface of the caudal horn of the medial meniscus (MM) beside the femoral attachment of the caudal cruciate ligament (CaCl). (d) Middle of the axial side of the medial femoral condyle (MFC) beside the medial side of the meniscofemoral ligament (MFL) covered with extensive synovial membrane (S). (e) Most proximal part of axial side of the medial femoral condyle (MFC) beside the termination of the meniscofemoral ligament (MFL) which was covered with synovial membrane (S).

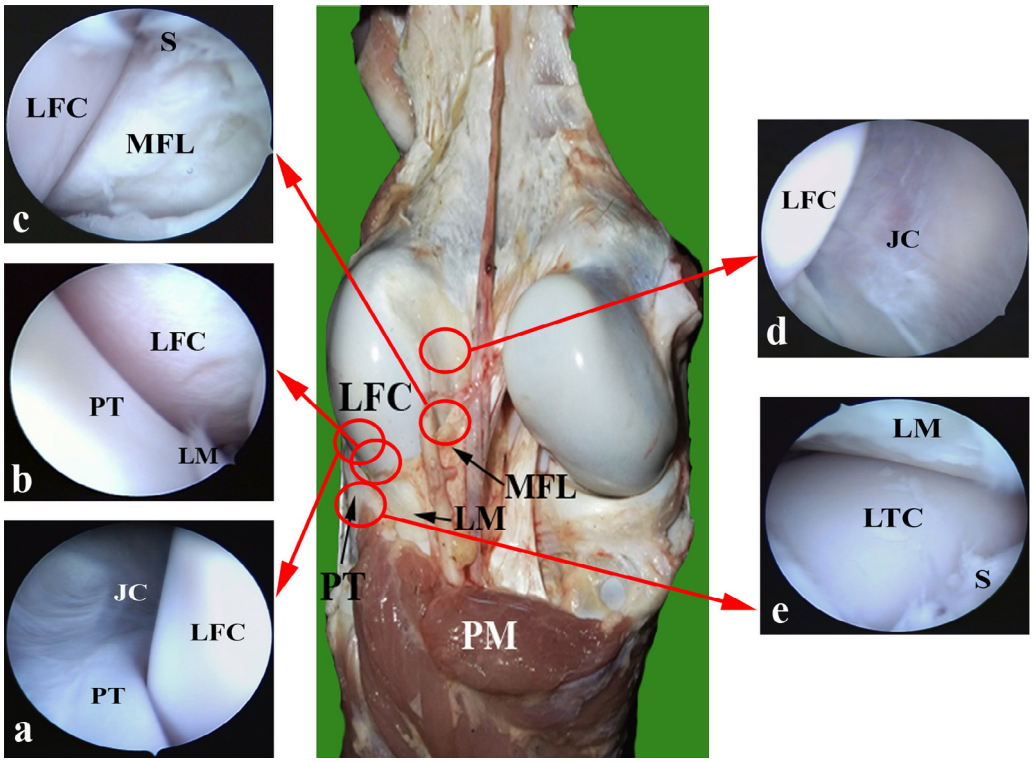

Fig. 7. Arthroscopic views of the proximal (a, b, c, d) and distal pouches (f) of the caudal compartment of the lateral femorotibial joint approach in Fig. 3B. Visual areas of the arthroscope identified using red circles on gross dissection of the caudal aspect of the left stifle joint; (LFC) lateral femoral condyle; (LM) caudal horn of the lateral meniscus; (PM) popliteus muscle; (PT) popliteal tendon; (MFL) meniscofemoral ligament. (a) Abaxial side of the lateral femoral condyle (LFC) beside the popliteal tendon (PT) and the joint cavity (JC). (b) Distal articular surface of the lateral femoral condyle (LFC); caudal horn of the lateral meniscus (LM) and the popliteal tendon (PT). (c) Middle of the axial side of the lateral femoral condyle (LFC); lateral side of the meniscofemoral ligament (MFL) covered with extensive synovial membrane (S). (d) Most proximal part of axial side of the lateral femoral condyle (LFC) and the joint cavity (JC). (e) Distal articular surface of the caudal horn of the lateral meniscus (LM) over the proximal articular surface of the lateral tibial condyle (LTC) lined with synovial membrane (S).

the medial femoral trochlear ridge (Fig. 4b). Moving the arthroscope in a semi-circular lateral direction following the articular contour between the trochlea and patella while rotating of the arthroscope around its longitudinal axis, the proximal portion of the medial femoral trochlear ridge, the medial aspect of the patella, the femoral inter-trochlear groove, the central and lateral articular surfaces of the patella, the lateral femoral trochlear ridge and the synovial membrane lining the lateral FP cul-de-sac were sequentially explored (Figs. 4b–e). The lateral femoral trochlear ridge was identified and evaluated from proximal to distal by moving the field of view distad with slight withdrawal action until the synovial reflection at the most distal end of the trochlear ridge was observed (Fig. 4f).

The articular surfaces of the patella and the inter-trochlear groove were observed by withdrawing the arthroscope (Fig. 4g). As withdrawal was continued, the suprapatellar pouch disappeared and the patellar apex and inter-trochlear groove were then viewed. The medial trochlear ridge and patella were observed by rotating the arthroscope around its longitudinal axis and directing the field of view towards the medial aspect of the joint. The medial trochlear ridge was explored from distal to proximal by directing the field of view proximad and introducing the arthroscope deeper into the joint with gradual flexion of the joint. The synovial membrane reflection medial to the medial trochlear ridge was inspected by withdrawing the arthroscope along the medial trochlear ridge, returning to the original view of the patella and medial trochlear ridge. Finally, the proximal synovial recess of the suprapatellar pouch (Fig. 4h) was inspected by increasing the intensity of illumination to its maximum and using a semi-circular movement of the arthroscope from proximomedial to proximolateral starting at the proximal edge of the medial trochlear ridge.

Cranial MFT compartment

To explore the cranial MFT joint, the arthroscope was withdrawn to the inter-condylar eminence and the axial side of the medial femoral condyle and the tibial attachment of the cranial cruciate ligament were recognized lateral to the eminence (Fig. 8a). A valgus stress was applied to the tibia in relation to the femur. Then by moving the arthroscope in a semi-circular distomedial direction following the articular contour of MFT joint, the cranial ligament of the medial meniscus, the cranial portion of the medial meniscus, the articular surface of the medial tibial condyle and the abaxial side of the medial femoral condyle were identified (Fig. 8b). The arthroscope was rotated around its longitudinal axis directing the field of view proximad to explore the abaxial side of the medial femoral condyle and the MFT cul-de-sac (Figs. 8c,d). Moving the arthroscope from the proximomedial to the proximolateral aspect of the MFT compartment allowed examination of the cranial and axial aspects of the medial femoral condyle and the femoral attachment of the caudal cruciate ligament (Fig. 8e) then the arthroscope was returned to the inter-condylar eminence.

Cranial LFT compartment

The arthroscope was advanced directly in a caudolateral direction from the inter-condylar eminence towards the cranial LFT joint. In three cadavers the synovial septum was penetrated to access the

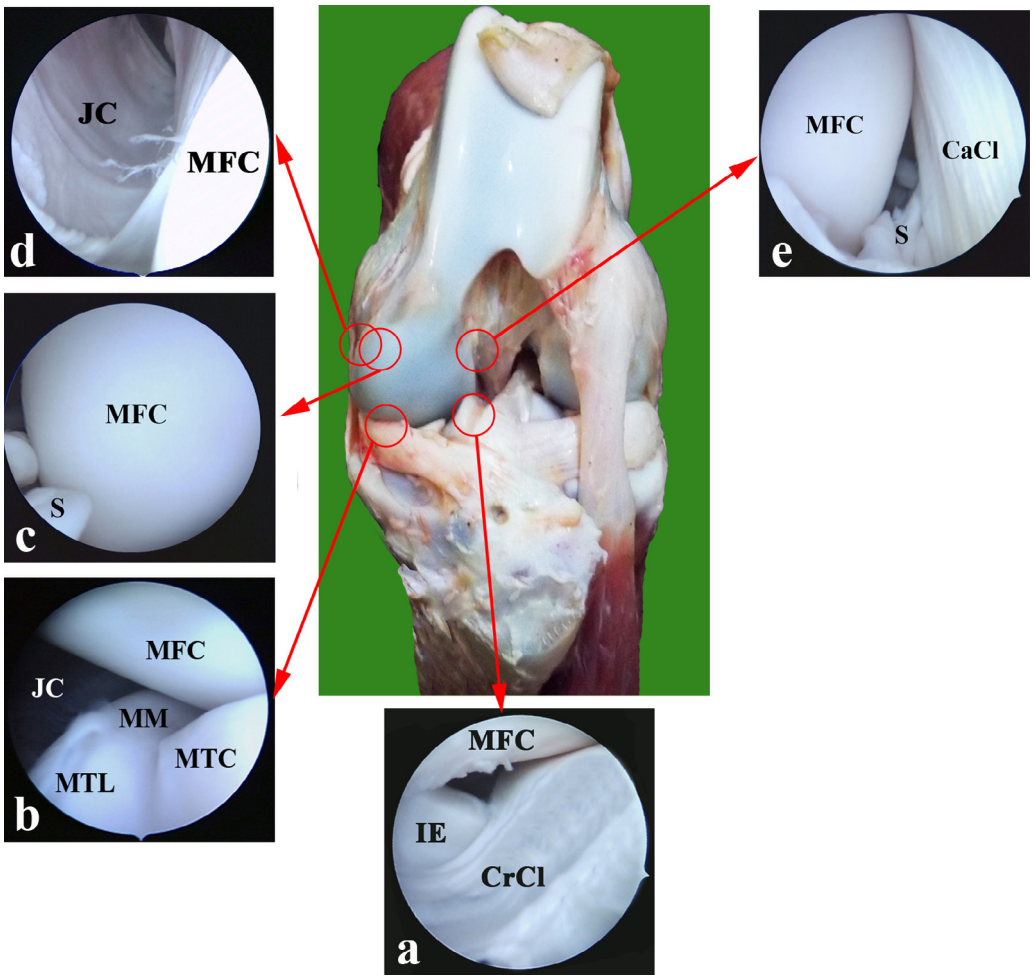

Fig. 8. Arthroscopic views of the cranial compartment of the medial femorotibial joint (a, b, c, d, e) using the craniomedial arthroscopic approach in Fig. 2A. Visual areas of the arthroscope identified with red circles on gross dissection of the cranial aspect of the left stifle joint. (a) Disto-axial side of the medial femoral condyle (MFC) over the proximal aspect of the inter-condylar eminence (IE) with the tibial attachment of the cranial cruciate ligament (CrCl). (b) Abaxial side of the articular surface of the medial femoral condyle (MFC) over the cranial horn of the medial meniscus (MM) with its meniscotibial ligament (MTL); proximal articular surface of medial tibial condyle (MTC); joint cavity (JC). (c) Close-up view of the arthroscope on the proximo-abaxial side of the medial femoral condyle (MFC) with extensive synovial membrane (S). (d) Close-up view of the arthroscope on the most proximo-abaxial side of the medial femoral condyle (MFC) and the medial cul-de-sac of the cranial femorotibial joint (JC). (e) Axial side of the medial femoral condyle (MFC) beside the femoral attachment of the caudal cruciate ligament (CaCl) with extensive synovial membrane (S).

cranial pouch of the LFT joint. The arthroscope was rotated until the axial aspect of the lateral femoral condyle (starting point) and the lateral margin of the lateral meniscus were identified (Fig. 9a). The arthroscope was rotated around its longitudinal axis directing the field of view distad to follow the curvature of the articulation between the lateral femoral condyle and the lateral meniscus to explore: the cranial end of the lateral meniscus, the cranial ligament of the lateral meniscus, the cranial aspect of the lateral femoral condyle, the lateral tibial condyle and the long digital extensor tendon under the synovial membrane and within the sulcus muscularis of the tibia (Fig. 9b). Further lateral insertion and rotation of the arthroscope allowed examination of the abaxial side of the lateral meniscus, abaxial aspect of the lateral femoral condyle as well as the popliteal tendon within its synovial diverticulum (Fig. 9c). Then the arthroscope was rotated and the field of view was directed proximad to explore the abaxial side of the lateral femoral condyle and the lateral cul-de-sac (Fig. 9d).

Caudal MFT compartment

To explore the caudomedial FT compartment, the arthroscope was directed axially, cranially, and slightly proximally from the described portal position aiming towards the axial aspect of the lateral femoral condyle until the abaxial caudal aspect of the medial femoral condyle was identified as a starting point (Fig. 6a). The arthroscope was rotated around its longitudinal axis directing the field of view distad to follow the curvature of the caudal MFT articulation to explore the caudal aspect of the medial femoral condyle and the caudal abaxial aspect of the caudal horn of the medial meniscus (Fig. 6b). Further insertion of the arthroscope with proximo-axial rotation allowed examination of the axial side of the caudal horn of the medial meniscus, axial side of the medial femoral condyle, femoral attachment of the caudal cruciate ligament and the meniscofemoral ligament (Figs. 6c,d). The arthroscope was advanced proximally to investigate the proximo-axial side of the medial femoral condyle and the meniscofemoral ligament (Fig. 6e).

Caudal LFT compartment

To approach the proximal caudolateral compartment, the arthroscope was introduced from the described portal position aiming towards the axial aspect of the medial femoral condyle and parallel to the tibial plateau until the abaxial aspect of the lateral femoral condyle was identified (Fig. 7a). The arthroscope was rotated around

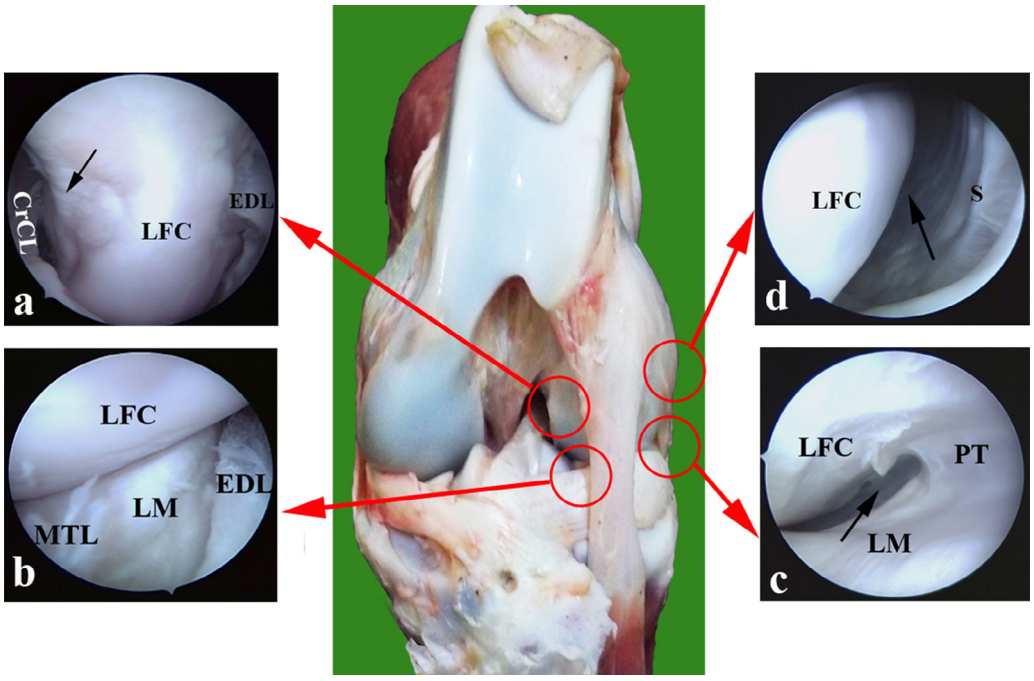

Fig. 9. Arthroscopic views of the cranial compartment of the lateral femorotibial joint (a, b, c, d) using the craniomedial arthroscopic approach in Fig. 2B. Visual areas of the arthroscope identified with red circles on gross dissection of the cranial aspect of the left stifle joint. (a) Proximo-axial part of the lateral condyle of the femur (LFC) and the cranial cruciate ligament (CrCL) that could be easily demonstrated medial to the axial part of the lateral femoral condyle (black arrow) and the long digital extensor tendon (EDL). (b) Disto-axial part of the lateral femoral condyle (LFC); cranial horn of the lateral meniscus (LM) with its meniscotibial ligament (MTL) and villous synovial membrane over the long digital extensor tendon (EDL). (c) Disto-abaxial aspect of the lateral femoral condyle (LFC); cranial horn of the lateral meniscus (LM); synovial diverticulum within the sulcus muscularis of the tibia (black arrow) and the popliteal tendon (PT). (d) Proximo-abaxial side of lateral femoral condyle (LFC) and the synovial joint capsule (S) lining the lateral cul-de-sac of the cranial femorotibial joint (black arrow).

its longitudinal axis directing the field of view distad to follow the curvature of the caudal LFT articulation to explore the popliteal tendon and the caudal horn of the medial meniscus (Fig. 7b). Further insertion and rotation of the arthroscope proximad permitted examination of the axial side of the lateral femoral condyle, meniscofemoral ligament and the proximo-axial side of the lateral femoral condyle (Figs. 7c,d).

To explore the distal pouch, the arthroscopic sleeve with the blunt obturator was advanced through the same portal used for the proximal pouch but directed slightly distal. Movement of the arthroscope within the distal pouch was limited; however, the caudal horn of the lateral meniscus and the lateral tibial condyle could be examined (Fig. 7e).

Discussion

The present study described the surgical technique and normal findings of the arthroscopic approaches to the cranial and caudal compartments of the stifle joint in cattle. Arthroscopic visualization of the MFT, LFT and FP joints was accomplished in a systematic order through a craniomedial single skin incision. The anatomical landmarks used to insert the scope into the MFT joint were similar to those used in South American camelids (Pentecost et al., 2012), sheep (Modesto et al., 2014) and cattle (Nichols and Anderson, 2014). During the anatomical study, palpation and identification of the medial and middle patellar ligaments, tibial plateau and patellar apex allowed localization of the craniomedial skin portal. However, it was difficult to palpate the collateral ligaments and the lateral patellar ligament was completely blended with the biceps femoris tendons, thus making localization of the craniolateral portal difficult. Similar findings were reported in the horse (Vinardell et al., 2008), sheep (Modesto et al., 2014) and cattle (Nichols and Anderson, 2014).

The craniomedial approach we used allowed a systematic exploration of the clinically important structures within the FP joint. The medial arthroscopic approach to the FP joint has been reported in the horse (Martin and McIlwraith, 1985), South American camelids (Pentecost et al., 2012) and cattle (Nichols and Anderson, 2014). The proximomedial femoral trochlear ridge was identified as a landmark and the arthroscope was advanced proximolaterally, distolaterally, distomedially and finally returned to the starting point to explore the suprapatellar pouch, thus allowing a consistent evaluation of the medial and lateral structures of the FP joint. In sheep (Modesto et al., 2014) and cattle (Nichols and Anderson, 2014) the FP joint was evaluated from the lateral approach, while in South American camelids the medial portal was used to evaluate the medial aspect and the lateral portal was used to explore the lateral aspect of the FP joint (Pentecost et al., 2012).

In our study, passing the arthroscope directly under the patella was associated with iatrogenic lesions caused by the metal rim of the arthroscopic sleeve. Lesions on the patellar apex were caused by trying to manipulate the obturator under the patella. Extension of the stifle to about 120° and gentle manipulation of the arthroscope beneath the patella were required to avoid iatrogenic damage of the patellar apex, as the patella in cattle is elongated and more pointed than in horse (Budras et al., 2003; Dyce et al., 2010). Some difficulty was encountered during examination of the distal aspect of the joint due to abundant synovium. This is in agreement with a previous study in cattle, where it was difficult to evaluate the distal aspect of the trochlear ridges without exiting the joint (Nichols and Anderson, 2014). In that study the FP joint was explored while the leg was extended, whereas in our study, fluid distension and gradual joint flexion (90°) allowed a consistent evaluation of the distal aspect of the trochlear ridges.

In the present study, exploration of the cranial FT joints was achieved in a systematic order commencing from an anatomic landmark in each compartment. A similar technique was described for the cranial FT joints in horse (Moustafa et al., 1987). However,

because the medial and lateral FT pouches communicate with each other in 57% of cattle (Desrochers et al., 1996), we found that, in most instances, moving from the medial to the lateral pouch of the cranial FT joints did not require resection of the synovial septum as in the horse. In a previous study, two arthroscopic portals were necessary to evaluate the cranial FT joints in cattle; the craniomedial approach was required to evaluate the axial side and the craniolateral approach was needed to evaluate the abaxial side of the FT joints (Nichols and Anderson, 2014). The systematic arthroscopic technique we describe here allowed a satisfactory examination of the cranial FT joints in all cadaveric stifles.

It was possible to evaluate the axial and abaxial sides of the cranial FT compartments via the craniomedial approach. The intercondylar eminence, medial and lateral femoral condyles, cranial ligaments of the menisci, cruciate ligaments, popliteal tendon and the long digital extensor tendon were evaluated. The lateral meniscus was efficiently evaluated, while the medial meniscus required specific joint manipulation as it was firmly attached to the medial collateral ligament. In order to obtain better observation of the medial meniscus, a valgus stress was applied to the tibia in relation to the femur similar to an approach described for the stifle joint of sheep (Modesto et al., 2014).

The caudal aspect of the femoral condyles, the caudal aspect of menisci and the caudal attachments of the cruciate ligaments could not be evaluated in any of the stifles we examined through the cranial FT joint approaches. Similar findings were reported in South American camelids (Pentecost et al., 2012), cattle (Nichols and Anderson, 2014) and sheep (Modesto et al., 2014). A caudal approach to the FT joints was required to evaluate those structures.

To our knowledge this is the first study describing the arthroscopic approach and the intra-articular anatomy of the caudal pouches of the FT joints in cattle. The technique described in our study shared some similarity with the caudal approach described in the horse (Watts and Nixon, 2006) in regard to the location of arthroscopic portals; however, in horse the caudolateral FT joint was entered more caudally and resulted in damage of the common peroneal nerve.

The caudal approaches to the medial and lateral FT joints did not cause damage to either the neurovascular structures or the femoral condyles. Limb flexion was critical to avoid damage of the common peroneal nerve. During cadaver limb dissection, the common peroneal nerve was observed about 3 cm caudal to the lateral collateral ligament. Flexion of the limb as well as joint distension during arthroscopy displaced the nerve to about 7–8 cm caudal to the lateral collateral ligament, meaning that the nerve could be avoided during joint entry.

The caudomedial approach allowed observation of the caudal portion of the medial femoral condyle and the caudal horn of the medial meniscus, caudal cruciate ligament and the meniscofemoral ligament. Exploration of the proximal caudolateral pouch offered good visibility of the lateral femoral condyle and the lateral meniscus. The distal caudolateral pouch was poorly explored due to its size providing a limited examination of the caudal tibial plateau and popliteal tendon behind the synovial lining. Similar findings have also been reported in the caudal FT joints of horses (Watts and Nixon, 2006) and sheep (Modesto et al., 2014).

In the present study, peri-articular fluid accumulation was common especially during exploration of the caudal FT compartments due to the distance between the skin and the joint. Despite this subcutaneous and intramuscular fluid accumulation, adequate joint distention could be maintained, however manipulation of the arthroscope and instruments was made more difficult because of the increased soft tissue thickness. Joint over distension and repeated joint penetration should be avoided to minimize periportal fluid extravasation.

A possible limitation of our study includes the relatively low number of stifles evaluated. In addition, exploration of the caudal pouches of the FT joints remained a challenge. Creation of a second instrumentation portal in the caudal FT compartments will be a limited option due to small size of the joint, depth of the joint from the skin surface and the risk of common peroneal nerve damage.

We demonstrated that the three cranial pouches of the stifle joint may be approached via a single skin incision. Explorations of both caudal compartments remain a challenge due to their size and anatomical features. The technique described allowed visualization of the most clinically relevant structures of the cranial and caudal compartments of the stifle joint in cattle.

Conclusions

Arthroscopic evaluation of the stifle joint in cattle allowed a good overall view of the most clinically relevant intra-articular structures. Information gained from these techniques will improve the clinician's ability to manage stifle injuries in cattle. Further investigations are needed to evaluate the diagnostic, therapeutic and prognostic applications of arthroscopy for bovine stifle pathology.

Conflict of interest statement

None of the authors of this paper has a financial or personal relationship with other people or organizations that could inappropriately influence or bias the content of the paper.

References

Ashdown, R.R., Done, S., 1984. Topographische Anatomie der Wiederkäuer. Enke, Stuttgart, pp. 36–157.
Budras, K.D., Habel, R.E., Wünsche, A., Buda, S., 2003. Bovine Anatomy, An Illustrated Text, 1st Ed. Schlütersche and Co. KG, Hannover.
Desrochers, A., St-Jean, G., Cash, W., Hoskinson, J.J., DeBowes, R.M., 1996. Characterization of anatomic communication between the femoropatellar joint and lateral and medial femorotibial joints in cattle, using intra-articular latex, positive contrast arthrography, and fluoroscopy. American Journal of Veterinary Research 57, 798–802.
Ducharme, N.G., Stanton, M.E., Ducharme, G.R., 1985. Stifle lameness in cattle at two veterinary teaching hospitals: A retrospective study of forty-two cases. Canadian Veterinary Journal 26, 212–217.
Dyce, K.M., Wensing, C.J.G., 1971. Essentials of Bovine Anatomy. Lea and Febiger, Philadelphia.
Dyce, K.M., Sack, W.O., Wensing, C.J.G., 2010. Textbook of Veterinary Anatomy, 4th Ed. Saunders Elsevier, St. Louis.
Ehlert, A., Ferguson, J., Gerlach, K., 2011. Magnetic resonance imaging and cross-sectional anatomy of the normal bovine tarsus. Anatomia, Histologia, Embryologia 40, 234–240.
Gaughan, E.M., 1996. Arthroscopy in food animal practice. Veterinary Clinics of North America Food Animal Practice 12, 233–247.
Honnas, C.M., Zamos, D.T., Ford, T.S., 1993. Arthroscopy of the coxofemoral joint of foals. Veterinary Surgery 22, 115–121.
Hurtig, M.B., 1985. Recent developments in the use of arthroscopy in cattle. Veterinary Clinics of North America Food Animal Practice 1, 175–193.
Kofler, J., 1999. Ultrasonographic examination of the stifle Region in cattle – Normal appearance. The Veterinary Journal 158, 21–32.
Kofler, J., Geissbuehler, U., Steiner, A., 2014. Diagnostic imaging in bovine orthopedics. Veterinary Clinics of North America Food Animal Practice 30, 11–53.
Lardé, H., Nichols, S., 2014. Arthroscopy in cattle: Technique and normal anatomy. Veterinary Clinics of North America Food Animal Practice 30, 225–245.
Lee, K., Yamada, K., Tsuneda, R., Kishimoto, M., Shimizu, J., Kobayashi, Y., Furuoka, H., Matsui, T., Sasaki, N., Ishii, M., et al., 2009. Clinical experience of using multidetector-row CT for the diagnosis of disorders in cattle. Veterinary Record 165, 559–562.
Lopez, M.J., Wilson, D., Markel, M., 1996. Ligament injury in the bovine stifle. Compendium on Continuing Education for the Practicing Veterinarian 18, 189–198.
Marino, D.J., Loughin, C.A., 2010. Diagnostic imaging of the canine stifle: A review. Veterinary Surgery 39, 284–295.
Martin, G.S., McIlwraith, C.W., 1985. Arthroscopic anatomy of the equine femoropatellar joint and approaches for treatment of osteochondritis dissecans. Veterinary Surgery 14, 99–104.
Modesto, R.B., Mansmann, K.A., Schaer, T.P., 2014. Arthroscopy of the normal cadaveric ovine femorotibial joint: A systematic approach to the cranial and caudal compartments. Veterinary and Comparative Orthopaedics and Traumatology 27, 387–394.
Moustafa, M.A.I., Boero, M.J., Baker, G.J., 1987. Arthroscopic examination of the femorotibial joints of horses. Veterinary Surgery 16, 352–357.

Munroe, G.A., Cauvin, E.R., 1994. The use of arthroscopy in the treatment of septic arthritis in two Highland calves. British Veterinary Journal 150, 439–449.
Necas, A., Srnec, R., Kecova, H., 2002. Diagnostic reliability of stifle arthroscopy of pathological changes in cruciate deficient knee. Acta Veterinaria Brno 71, 249–254.
Nichols, S., Anderson, D.E., 2014. Determination of the normal arthroscopic anatomy of the femoropatellar and cranial femorotibial joints of cattle. Canadian Veterinary Journal 55, 232–239.
Nickel, R., Schummer, A., Seiferle, E., 1985. The Anatomy of the Domestic Animals. Verlag Paul Parey Berlin, Hamburg. Springer-Verlag, New York.
Nuss, K., Schnetzler, C., Hagen, R., Schwarz, A., Kircher, P., 2011. Clinical application of computed tomography in cattle. Tierärztliche Praxis Ausgabe G: Grosstiere – Nutztiere 39, 317–327.
Pentecost, R., Niehaus, A., 2014. Stifle disorders: Cranial cruciate ligament, meniscus, upward fixation of the patella. Veterinary Clinics of North America Food Animal Practice 30, 265–281.
Pentecost, R.L., Niehaus, A.J., Santschi, E., 2012. Arthroscopic approach and intraarticular anatomy of the stifle in South American camelids. Veterinary Surgery 41, 458–464.
Plesman, R., Gilbert, P., Campbell, J., 2013. Detection of meniscal tears by arthroscopy and arthrotomy in dogs with cranial cruciate ligament rupture: A retrospective, cohort study. Veterinary and Comparative Orthopaedics and Traumatology 26, 42–46.
Siegrist, A., Geissbuehler, U., 2011. Radiographic examination of cattle. Tierärztliche Praxis Ausgabe G: Grosstiere – Nutztiere 39, 331–340.
Trostle, S.S., Nicoll, R.G., Forrest, L.J., Markel, M.D., 1997. Clinical and radiographic findings, treatment, and outcome in cattle with osteochondrosis: 29 cases (1986–1996). Journal of the American Veterinary Medical Association 211, 1566–1570.
Tryon, K.A., Farrow, C.S., 1999. Osteochondrosis in cattle. Veterinary Clinics of North America Food Animal Practice 15, 265–274.
Vinardell, T., David, F., Morisset, S., 2008. Arthroscopic surgical approach and intra-articular anatomy of the equine suprapatellar pouch. Veterinary Surgery 37, 350–356.
Watts, A.E., Nixon, A.J., 2006. Comparison of arthroscopic approaches and accessible anatomic structures during arthroscopy of the caudal pouches of equine femorotibial joints. Veterinary Surgery 35, 219–226.